FT-Raman and FT-IR spectroscopic study of synthetic Mg/Zn/Al-hydrotalcites

J. Theo Kloprogge*, Leisel Hickey and Ray L. Frost

Inorganic Materials Research Program

Queensland University of Technology, GPO Box 2434, Brisbane Q 4001, Australia.

Published as:
Kloprogge, J.T., Frost, R.L. and Hickey, L. (2004) FT-Raman and FT-IR spectroscopic study of the local structure of synthetic Mg/Zn/Al-hydrotalcites. Journal of Raman Spectroscopy, 35, 967-974.

ABSTRACT

Synthetic Mg/Zn/Al-hydrotalcites with atomic ratios of 6/0/2, 4/2/2, 2/4/2 and 0/6/2 have been characterised by FT-Raman and FT-IR spectroscopy. "Al-OH" IR translation modes are observed at 419, 427, 559, 616 and 771 cm^{-1} with 2 corresponding Raman bands at 465-477 and 547-553 cm^{-1}. "Mg-OH" IR translation modes are found at 412, 559 and 616 cm^{-1} with equivalent Raman bands at 464-477 and 547-553 cm^{-1}. The "Zn-OH" IR translation mode is found at 445 cm^{-1} and the Raman modes around 450 and 495 cm^{-1}. The CO_3^{2-} group is identified by the ν_1(IR) at 1112 cm^{-1} and a doublet in the Raman around 1045-1055 and 1060 cm^{-1}. The ν_2(IR) is observed at 874 cm^{-1}. The ν_3(IR) is a doublet at 1359 and 1381 cm^{-1}. The ν_4 is observed in both IR and Raman around 670 cm^{-1} and 695-715 cm^{-1}, respectively. In the OH-deformation region a doublet is observed for "Al-OH" at 955 and 1033 cm^{-1} in the IR. The "Zn-OH" IR deformation mode is observed at 1462 cm^{-1}. H_2O is characterised by a bending mode at 1632 cm^{-1} and an H-bonded interlayer H_2O mode at 3266 cm^{-1} with a Raman band between 3244 and 3271 cm^{-1}. The OH-stretching region is characterised by 3 bands in the Raman around 3355-3360, 3440-3455 and 3535-3580 cm^{-1}. One band is observed in the IR at 3471 cm^{-1}.

Key words – FT-IR spectroscopy, FT-Raman, hydrotalcite, hydroxycarbonate, layered double hydroxide, LDH, synthesis

INTRODUCTION

Hydrotalcites are in the literature also known as anionic clays, due to their layered structure with a charge opposite to that of cationic clays like smectites. Hydrotalcites or layered double hydroxides can be visualised as positively charged hydroxide layers comparable to the hydroxide layers in brucite in which a part of the Mg^{2+} is substituted by a trivalent metal with a similar radius like Al^{3+} or Fe^{3+} (pyroaurite-sjögrenite). The higher charge of the trivalent cation imposes an overall positive charge on the brucite-like layer, which is charge compensated mostly by hydrated interlayer anions [1-4]. In synthetic hydrotalcites a broad range of compositions are possible of the type $[M^{II}_{1-x}M^{III}_{x}(OH)_2][A^{n-}]_{x/n}.yH_2O$, where M^{II} and M^{III} are the di- and trivalent cations in the octahedral positions within the hydroxide layers with x normally between 0.17 and 0.33. A^{n-} is an exchangeable interlayer anion.

Coprecipitation is probably the most reliable and reproducible techniques for the preparation of hydrotalcites. It allows homogeneous precursors to be used as starting materials, where two or more elements are intimately mixed together. For coprecipitation it is necessary to work under conditions of supersaturation mostly achieved by variation in pH [5]. Most of the metals known to be incorporated in synthetic hydrotalcites form hydroxide precipitates around pH values of 8 to 10. In this study the high supersaturation route explored by e.g. Reichle and coworkers [6-8] was used for the preparation of two and three metal hydrotalcites containing Mg^{2+}, Zn^{2+}, and Al^{3+} as cations in a molar ratios of 6/0/2, 4:2:2, and 2/4/2 with CO_3^{2-} as interlayer anion. The addition of a second divalent metal like Zn is important for applications in a number of polymers (PVC, PP, PE) as anion scavengers and UV- and heat-stabilisers [9].

Infrared and very rarely Raman spectroscopy has been applied for the study of hydrotalcites with different cations, the anionic pillaring of hydrotalcites and the thermal decomposition of hydrotalcites, but mainly for the study of exchangeable anions such as CO_3^{2-}, Cl^-, ClO_4^-, NO_3^-, SO_4^{2-}, CrO_4^{2-} and $SiO(OH)_3^-$ [6,10-15] and larger polyoxometalate ions with e.g the Keggin structure or $Fe(CN)_6^{n-}$ [16-18]. Each of these anions shows specific infrared bands. Carbonate for example is characterised by a strong double peak around 1360 and 1400 cm^{-1} and peaks at 880 and 680 cm^{-1} [19].

Many variations in divalent/trivalent cation combinations have been reported for both natural and synthetic hydrotalcites [5]. One of these variations in cations comprise the variety known as takovite, a hydrotalcite structure in which Mg is replaced by Ni [12,20-25]. The infrared spectra from hydrotalcites with Mg partly or completely replaced by Co, Mn, and Zn have also been briefly reported [22-30]. Kooli *et al*., [26] indicated that the addition of Zn in the Mg/Al hydrotalcite composition did not result in any important variation in the bands except for those weak bands characteristic of the carbonate ion still present in their sulphate system. However detailed descriptions of the influence of different cations on the Raman and IR spectra, especially on the lattice region, of hydrotalcite have not been described. In situ studies of anionic clays, e.g. upon decomposition, are even more scarce. Recently infrared emission spectroscopy and thermal analysis-mass spectrometry have been used in this field of research to study the dehydration, dehydroxylation and decarbonation of hydrotalcite [25,27,28].

In order to contribute to a better understanding of the two- and three-metal hydrotalcite structures, a FT-Raman in combination with FT-IR spectroscopic study was undertaken followed by detailed band component analysis on a well defined hydrotalcites with a 3/1 (Mg+Zn)/Al atomic ratio and various Mg/Zn atomic ratios.

EXPERIMENTAL

The hydrotalcites with theoretical compositions of $Mg_6Al_2(OH)_{16}CO_3.nH_2O$, $Mg_4Zn_2Al_2(OH)_{16}CO_3.nH_2O$, and $Mg_2Zn_4Al_2(OH)_{16}CO_3.nH_2O$ were synthesised by the slow simultaneous addition (approximately 1 ml/minute) of appropriate mixed aluminum-magnesium- zinc nitrate (total nitrate concentration 1.0 M) solutions and a NaOH solution (2.0 M) with 0.25 M Na_2CO_3 under vigorous stirring buffering the pH at approximately 10. The solid products were washed to eliminate excess salt and separated from the suspension by centrifugation. This was repeated five times followed by drying overnight at 60°C. For comparison a pure Zn/Al hydrotalcite described in a related study has been included in this study [29].

The nature of the resulting material was checked by X-ray powder diffraction (XRD). The XRD analyses were carried out on a Philips wide angle PW 1050/25 vertical goniometer equipped with a graphite diffracted beam monochromator. The d-values and intensity measurements were improved by application of an in-house developed computer aided divergence slit system enabling constant sampling area irradiation (20 mm long) at any angle of incidence. The goniometer radius was enlarged to 204 mm. The radiation applied was CoKα from a long fine focus Co tube operating at 35 kV and 40 mV. The samples were measured at 50 % relative humidity in stepscan mode with steps of 0.02° 2θ and a counting time of 2s. The chemical composition in terms of metal contents was determined by Inductively Coupled Plasma – Atomic Emission Spectrometry (ICP-AES).

The Fourier Transform Raman spectroscopy (FT-Raman) analyses were performed on powder samples pressed in a sample-holder suitable for the spectrometer using a Perkin Elmer System 2000 Fourier transform spectrometer equipped with a Raman accessory comprising a Spectron Laser Systems SL301 Nd:YAG laser operating at a wavelength of 1064 nm. Spectral manipulation such as baseline adjustment, smoothing and normalisation were performed using the Spectracalc software package GRAMS (Galactic Industries Corporation, NH, USA). Band component analysis was carried out using the peakfit software package by Jandel Scientific. Lorentz-Gauss cross product functions were used throughout and peak fitting was carried out until the squared correlation coefficients with r^2 greater than 0.995 were obtained.

The hydrotalcites were oven dried at 60°C overnight to remove any adsorbed water and stored in a desiccator before measurement in the FT-IR spectrometer. The sample (1mg) was finely ground for one minute, combined with oven dried spectroscopic grade KBr having a refractive index of 1.559 and a particle size of 5-20 μm (250mg) and pressed into a disc using 8 tonnes of pressure for five minutes under vacuum. The spectrum of each sample was recorded in triplicate by accumulating 64 scans at 4 cm^{-1} resolution between 400 cm^{-1} and 4000 cm^{-1} using the Perkin-Elmer 1600 series Fourier transform infrared spectrometer equipped with a LITA detector. Data interpretation and manipulation were carried out using the Spectracalc software package GRAMS (Galactic Industries Corporation, NH, USA). Band component analysis was carried out using the peakfit software package by Jandel Scientific. Lorentz-Gauss cross product functions were used throughout and peakfitting was carried out until the squared correlation coefficients with r^2 greater than 0.995 were obtained.

RESULTS AND DISCUSSION

X-Ray diffraction

Fig. 1 shows the X-ray diffraction patterns of the various hydrotalcites. All samples only showed crystalline hydrotalcite without any impurities. Characteristic for these samples is the decrease in intensity and broadening of the basal reflections (00*l*) with increasing Zn-content indicating both a lower crystallinity and a smaller crystallite size. Both these observations are in agreement with transmission electron micrographs. It indicates that the incorporation of Zn leads to an increase in stress in the octahedral hydroxide layer in the hydrotalcite crystal structure, due to the difference in ionic radii between Mg^{2+} and Zn^{2+} as there are no differences in the bond lengths of the six M-OH bonds around a single octahedral site [3].

Chemical analysis

ICP-AES analysis of the hydrotalcite samples used in this study (Table 1) show a Al-content consistent with the theoretical composition. The Mg-contents of the pure Mg-endmember and the Mg/Zn/Al 4/2/2 are slightly lower than expected. The Zn-content in the Mg/Zn/Al 4/2/2 is slightly lower and higher, respectively, than one would expect based on the theoretical compositions. However, the differences in chemical compositions compared to the theoretical compositions are too small to discuss the changes in the infrared and Raman spectra based on actual compositions instead of the theoretical compositions. Therefore, in the rest of the paper the theoretical compositions will be used for the interpretation of the infrared and Raman spectra of the various samples.

FT-IR spectroscopy

Figure 3 shows the FT-IR spectrum in the region between 400 and 4000 cm^{-1} and the hydroxyl-stretching region of the $Mg_4Zn_2Al_2(OH)_{16}CO_3.nH_2O$ hydrotalcite (Mg/Zn/Al 4/2/2). The low-frequency region is characterised by a complex group of eight bands centred on 420 cm^{-1}. All the bands and their possible assignments are listed in Table 2. With the assignment it has to be kept in mind that most of the OH-groups are (when not at the edges of the crystals) triply coordinated. If the various metals in the hydrotalcites (Mg, Zn, Al) are distributed at random, it is rather unlikely that an OH-group is surrounded by three metal cations of the same kind. In most cases one OH-group will be coordinated by at least two different metal cations. This means that in the following text an assignment like “Al-OH” means that the vibration in question mostly resembles an Al-OH mode.

All the data from the band component analyses are tabulated in Table 3. Figure 2a depicts the band component analysis of this complex region revealing strong bands at 412, 419, 427, and 439 cm^{-1}. These bands are associated with M^{II}-O and M^{III}-OH bonds while the 419-cm^{-1} band is assigned to an M^{III}-OH translation mode comparable to the very weak 425-cm^{-1} band of bayerite ($Al(OH)_3$). The band at 412 cm^{-1} is assigned to the “Mg-OH” translation mode because of its occurrence in Zn-free natural hydrotalcites. Natural hydrotalcite also shows a very broad band at 465-430 cm^{-1} [30]. Others only reported a single band centred at 420 cm^{-1} without further details of the presence of other bands (*e.g.* [19,31]). The Zn/Al hydrotalcite prepared at a pH 14 shows a band around 440 cm^{-1}. This lead to the conclusion that the additional band observed at 444 cm^{-1} in comparison to Zn-free hydrotalcite

belongs to "Zn-OH" translation mode. This is also supported by the fact that ZnO has a similar broad band at 450 cm^{-1} [32] and $Zn(OH)_4^{2-}$ at 484 cm^{-1}. Similarly, a band at 460 cm^{-1} is observed for hydrozincite [30].

The region between 500 and 1200 cm^{-1} is characterised by eight bands (Fig. 2b). The bands at 558, 616, and 771 cm^{-1} are ascribed to "Al-OH" and "Mg-OH" translation modes comparable to those at 555, 625, and 764 cm^{-1} observed in natural bayerite and at 575-550, 690-640 cm^{-1} for brucite [30] (Table 1). The relatively broad bands at 955 and 1033 cm^{-1} have not been reported before for hydrotalcite. These bands, which were also observed in the Zn/Al-hydrotalcite, are absent in the spectrum of brucite, $Mg(OH)_2$, the structure from which hydrotalcite can be derived. However, in bayerite a doublet is observed at 970 and 1021 cm^{-1} leading to the possible assignment of a new type of Al-O bonds in hydrotalcite. The bands at 671, 874, and 1112 cm^{-1} are characteristic for the ν_4, ν_2 and ν_1 of the interlayer CO_3^{2-} group. Two bands very close together assigned to the ν_3 have been observed around 1359 and 1381 cm^{-1} (Fig. 2c), while in the literature one band is described around 1400 cm^{-1}. This may indicate that two different types of CO_3^{2-} are present in the interlayer of the hydrotalcite, possibly associated with the location near octahedra either containing Mg or Zn. Although the symmetric stretching modes ν_1 and ν_3 have not been described before, they are well known for other bicarbonate minerals. In bicarbonates the symmetry is lowered to C_{2v} and all 6 expected normal modes become active. In general for bicarbonates absorptions are found at 1700-1600 cm^{-1} (strong broad), near 1400 cm^{-1} (very strong), between 1000 and 950 cm^{-1} (medium, 2 or 3 bands), in the 850-800 cm^{-1} region (medium sharp) and between 720 and 650 cm^{-1} (medium, 1 or 2 bands) [30]. The very broad band in the 1700-1600 cm^{-1} region described for bicarbonates is not recognised in the hydrotalcite spectrum. However, when it is present it is obscured by the water-bending mode at 1632 cm^{-1}.

The region between 2700 and 3750 cm^{-1}, also known as the OH-stretching region, is characterised by very broad bands at 2938, 3266, and 3471 cm^{-1} (Fig. 2d). The 2938-cm^{-1} band is generally interpreted as the CO_3-H_2O bridging mode [10,33]. The 3266-cm^{-1} band is ascribed to H-bonded interlayer H_2O surrounding the interlayer anion. The strong band at 3471 cm^{-1} is ascribed to the metal-OH stretching mode. One can not discriminate between the various metals (Mg, Zn, Al) bonded to the OH groups in the IR spectrum.

FT-Raman spectroscopy

In order to come to a more detailed assignment of the various bands in the IR spectrum the Raman spectra of hydrotalcites with different Mg/Zn ratios have been collected. Figure 3 shows the Raman spectra with increasing Mg/Zn ratio from top to bottom.

In the region between 400 and 440 cm^{-1}, where seven IR bands are observed for hydrotalcite, no Raman bands can be observed. However for the single IR band at 445 cm^{-1} we now observe three different Raman bands around approximately 442-455, 465-475, and 494-497 cm^{-1}. Figure 4a shows an example of the band component analysis of a hydrotalcite with a Mg/Zn ratio of 2/4. The first band, which is both IR- and Raman-active can be ascribed to "Zn-OH" based on the analogy between hydrotalcite and the pure hydroxides. The next two bands are only Raman-active. The band around 465-475 cm^{-1} can be observed in all samples and must therefore be ascribed again to a combination of "Mg-OH" and "Al-OH". The last band, however, is not observed for the hydrotalcite without Zn, while the pure Zn/Al-hydrotalcite

exhibits a band at 500 cm^{-1}, and therefore this band around 495 cm^{-1} must be assigned to an OH-group strongly coordinated to Zn. A significant feature is that the band around 980 cm^{-1} assigned to "Al-OH" shows an increase in intensity with increasing Zn content in the hydrotalcite structure. A similar although less strong observation can also be made for the "Al-OH" or "Mg-OH" band around 550 cm^{-1}.

The interlayer CO_3^{2-} bands can be observed in the Raman spectra as a very weak and broad band at approximately 695 cm^{-1} (ν_4), and a strong and sharp band around 1060 cm^{-1} (ν_1). The ν_2 and ν_3 are only IR-active and not Raman-active. Band component analysis reveal that the sharp 1060-cm^{-1} band actually contains a second, much broader band at a slightly lower frequency (approximately 1055 cm^{-1}). Figure 5b shows the band component analysis of the hydrotalcite with Mg/Zn ratio of 2/4. In the IR spectrum only one band was observed at 1112 cm^{-1} instead. As with the double ν_3 band in the IR spectrum this may indicate the presence of two different positions for the interlayer CO_3^{2-} within the hydrotalcite structure.

The hydroxyl stretching region in the Raman spectra is complex compared to the IR spectra of hydrotalcite (Fig. 4b). In addition to the CO_3-H_2O bridging mode around 3000-3050 cm^{-1} and the H-bonded interlayer H_2O around 3250 cm^{-1}, there are now four different metal-OH stretching modes instead of the single one in the IR spectrum at 3471 cm^{-1}. New bands can be observed around 3355-3365 cm^{-1} and a relatively small band around 3560-3580 cm^{-1}. Figure 4b shows an example of the band component analysis of one of the samples. Table 4 shows that a general trend can be found in the relative intensities of the three bands. The band due to the interlayer water strongly increases with increasing Zn-content in the hydrotalcite structure. The first band around 3355-3365 cm^{-1} remains nearly constant (within the experimental error) with increasing Zn- and decreasing Mg-content. The band around 3450 cm^{-1} strongly decreases with decreasing Mg-content. However, none of these bands disappear in either the Mg- or the Zn-endmember hydrotalcite. So none of these bands can be ascribed to a single Mg-OH or Zn-OH stretching mode based on these observations. Crystallographically there are no differences in the bond lengths of the six M-OH bonds around a single octahedral site [3]. Therefore the differences are probably best explained by a combination of differences in the atomic weight of the three metal cations (Mg 24.3, Al 27.0 and Zn 65.4) and differences in bondstrengths. Changes in the chemical composition may as a consequence change the direction in which the OH groups are pointing in the hydrotalcite structure resulting in different stretching bands. The fact that the lowest and highest frequencies are only observed in the Raman spectra indicates a very symmetric environment.

CONCLUSIONS

The infrared and Raman spectra of synthetic hydrotalcites with different Mg/Zn ratios reveal complex spectra. Based on the differences in the spectra between the various hydrotalcites and comparison to the comparable hydroxides and hydroxycarbonates a much more detailed band assignment can be made than has been published before. "Al-OH" translation modes are observed at 419, 427, 559, 616 and 771 cm^{-1} in the IR spectra. Only two equivalent Raman bands are observed at approximately 465-477, 547-553 cm^{-1}. "Mg-OH" IR translation modes can be found at 412, 559 and 616 cm^{-1} with equivalent Raman bands at 464-477 and 547-553 cm^{-1}. Not in all cases a distinction can be made between "Mg-OH" or "Al-OH" translation modes. "Zn-OH" translation modes are found at 445 cm^{-1} (IR), around 450 cm^{-1} (Raman) and around 495 cm^{-1} (Raman). The interlayer CO_3^{2-} group is identified by the ν_1 IR mode at 1112

cm^{-1}, which is shown as a doublet in the Raman around 1045-1055 and 1060 cm^{-1}. The ν_2 mode is observed in the IR spectrum at 874 cm^{-1} but was not visible in the Raman spectra. The ν_3 mode is also a doublet in the IR spectrum at 1359 and 1381 cm^{-1} but again not visible in the Raman spectra. The ν_4 mode is observed in both the IR and Raman spectra around 670 cm^{-1} and 695-715 cm^{-1} respectively. In the OH-deformation region a doublet is observed for "Al-OH" at 955 and 1033 cm^{-1} in the IR spectrum, which are not observed in the Raman spectra. The "Zn-OH" deformation mode is observed as a single band around 1462 cm^{-1} in the IR spectrum. Water is characterised by a bending mode at 1632 cm^{-1} and an H-bonded interlayer H_2O mode at 3266 cm^{-1}. This last band is also seen in the Raman spectra between 3244 and 3271 cm^{-1}. The hydroxyl-stretching region is characterised by three different bands in the Raman spectra around 3355-3360, 3440-3455 and 3535-3580 cm^{-1}. Only one band is observed in the IR spectrum at 3471 cm^{-1}. The occurrence of three different bands in the OH-stretching region for a crystal structure which has only one M-OH bondlength is most probably due to the differences in atomic weight with increasing weight Mg<Al<Zn and differences in bondstrengths. These differences may cause differences in the direction in which the OH-groups are pointing in the hydrotalcite structure. The fact that the lowest and highest frequencies are observed only in the Raman spectra indicates a very symmetric environment.

ACKNOWLEDGMENTS

The financial and infra-structural support of the Queensland University of Technology, Centre for Instrumental and Developmental Chemistry is gratefully acknowledged.

REFERENCES

1. Allmann, R. *Acta Crystall. B* 1968**; 24**: 972.
2. Taylor, HFW. *Miner. Mag.* 1969**; 37**: 338.
3. Allmann, R. *Chimia* 1970**; 24**: 99.
4. Taylor, HFW. *Miner. Mag.* 1973**; 39**: 377.
5. Cavani, F, Trifirò, F, Vaccari, A. *Catal. Today* 1991**; 11**: 173.
6. Reichle, WT, Kang, SY, Everhardt, DS. *J. Catal.* 1986**; 101**: 352.
7. Reichle, WT. *Solid State Ionics* 1986**; 22**: 135.
8. Reichle, WT. *J. Catal.* 1985**; 94**: 547.
9. Dick, S, Schiessling, H. "Polymer applications of layered double hydroxides"; Euroclay 1999,, 1999, Krakow, Poland.
10. Miyata, S. *Clays Clay Miner.* 1975**; 23**: 369.
11. Miyata, S, Okada, A. *Clays Clay Miner.* 1977**; 25**: 14.
12. Evana, E, Marchidan, R, Manaila, R. *Bull. Soc. Chim. Belge* 1992**; 2**: 101.
13. Schutz, A, Biloen, P. *J. Solid State Chem.* 1987**; 68**: 360.
14. Kloprogge, JT, Frost, RL. Infrared and Raman spectroscopic studies of layered double hydroxides (LDHs). In *Layered Double Hydroxides: Present and Future;* Rives, V Ed.; Nova Science Publishers, Inc.: New York, 2001; pp. 139.
15. Kloprogge, JT, Wharton, D, Hickey, L, Frost, RL. *Amer. Miner.* 2002**; 87**: 623.
16. Wang, J, Tian, Y, Wang, RC, Colon, JL, Cearfield, A. *Mater. Res. Soc. Symp. Proc.* 1991**; 233**: 63.
17. Hansen, HCB, Koch, CB. *Clays Clay Miner.* 1994**; 42**: 170.
18. Idemura, S, Suzuki, E, Ono, Y. *Clays Clay Miner.* 1989**; 37**: 553.
19. Hernandez-Moreno, MJ, Ulibarri, MA, Rendon, JL, Serna, CJ. *Phys. Chem. Miner.* 1985**; 12**: 34.
20. Bish, DL, Brindley, GW. *Amer. Miner.* 1977**; 62**: 458.
21. Bish, DL. *Bull. Miner.* 1980**; 103**: 170.
22. Labajos, FM, Rives, V, Ulibarri, MA. *Spectrosc. Letters* 1991**; 24**: 499.
23. Ehlsissen, KT, Delahaye-Vidal, A, Genin, P, Figlarz, M, Willmann, P. *J. Mater. Chem.* 1993**; 3**: 883.
24. Kloprogge, JT, Frost, RL. *J. Solid State Chem.* 1999**; 146**: 506.
25. Kloprogge, JT, Frost, RL. *Appl. Catal. A* 1999**; 184**: 61.
26. Kooli, F, Kosuge, K, Hibino, T, Tsunashima, A. *J. Mater. Sci.* 1993**; 28**: 2769.
27. Kloprogge, JT, Frost, RL. *Phys. Chem. Chem. Phys.* 1999**; 1**: 1641.
28. Kloprogge, JT, Kristof, J, Frost, RL. *2001 a Clay Odyssey, Proceedings of the International Clay Conference, 12th, Bahia Blanca, Argentina, July 22-28, 2001* 2003: 451.
29. Kloprogge, JT, Hickey, LA, Frost, RL. *J. Solid State Chem.* 2004: Accepted.
30. Gadsden, JA *Infrared Spectra of Minerals and Related Inorganic Compounds*; Butterworths: England, 1975.
31. Kannan, S, Swamy, CS. *J. Mater. Sci. Letters* 1992**; 11**: 1585.
32. Ferraro, JR *Low Temperature Vibrations of Inorganic and Coordination Compounds*; Plenum Press: New York, 1971.
33. Titulaer, MK, Jansen, JBH, Geus, JW. *Clays Clay Miner.* 1994**; 42**: 249.

Table 1. Chemical analysis of the Mg/Zn/Al-hydrotalcites in elemental percentages and comparison to the theoretical values based on dry hydrotalcite $(MgZn)_6Al_2(OH)_{16}CO_3$.

element	hydrotalcite Mg/Zn/Al 6/0/2	Calculated Mg/Zn/Al 6/0/2	hydrotalcite Mg/Zn/Al 4/2/2	Calculated Mg/Zn/Al 4/2/2	hydrotalcite Mg/Zn/Al 2/4/2	Calculated Mg/Zn/Al 2/4/2
Al	9.22	10.2	7.23	8.8	7.82	7.8
Mg	21.26	27.4	12.84	15.8	7.00	7.0
Zn	0.22	0.0	19.81	21.3	42.48	37.6

Table 2. FT-IR and FT-Raman band positions of synthetic hydrotalcites compared to similar bands in related minerals and suggested interpretation.

FT-IR bands (cm^{-1}) hydrotalcite Mg/Zn/Al 4/2/2	FT-Raman bands (cm^{-1}) hydrotalcite Mg/Zn/Al 6/0/2	FT-Raman bands (cm^{-1}) hydrotalcite Mg/Zn/Al 4/2/2	FT-Raman bands (cm^{-1}) hydrotalcite Mg/Zn/Al 2/4/2	IR natural hydrotalcite Mg/Al 6/2 (Gadsden, 1975)	IR natural bayerite $Al(OH)_3$ (Gadsden, 1975)	IR natural brucite $Mg(OH)_2$ (Gadsden, 1975)	IR natural hydrozincite $2[Zn_5(CO_3)_2(OH)_6]$ (Gadsden, 1975)	Suggested assignment
400								Unknown
405								Unknown
412				412				“Mg-OH” translation
419								“Al-OH” translation
427					425 vw			“Al-OH” translation
433								Unknown
439								Unknown
444		452	443				460	“Zn-OH” translation
	476	476	477		458 sh	465-30 vs vb		“Al-OH” or “Mg-OH” translation
		496	494				520	“Zn-OH” translation
559	552	548	550	555	555 sh	575-50 b sh		“Al-OH” or “Mg-OH” translation
616					625 b sh	690-40 b sh		“Al-OH” or “Mg-OH” translation

672	694	694	695	650		710	ν_4 CO_3^{2-}
771				764 vs b			"Al-OH" translation
874				865	860 sh	837	ν_2 CO_3^{2-}
955	979	979	981		974 b	960	Doublet "Al-OH"
1033					1021		deformation
1112	1053	1044	1056			1050	ν_1 CO_3^{2-}
	1061	1060	1061			1070	
1359						1340	ν_3 CO_3^{2-}
1381				1400		1400	
1462						1515	"Zn-OH" deformation
1632				1650	1630 w b		H_2O bending
2938	3097	3006	3068		2900 w		CO_3-H_2O bridge
3266	3245	3261	3249		3290 m		H-bonded interlayer H_2O
	3358	3362	3366			3300	M-OH_1 stretch
3471	3454	3444	3445				M-OH_2 stretch
	3580	3562	3535	3575	3570 w		M-OH_3 stretch

Table 3. Band component analysis of the FT-IR spectrum of hydrotalcite with composition $Mg_4Zn_2Al_2(OH)_{16}CO_3.nH_2O$.

Band position (cm^{-1})	Band width (cm^{-1})	Relative intensity (%)
390-450 cm^{-1} region		
400	2	0.7
405	6	6.6
412	6	15.7
419	7	13.3
427	11	36.5
433	6	4.4
439	8	15.6
445	6	7.2
500-1250 cm^{-1} region		
559	34	3.2
616	58	9.0
672	61	15.9
771	139	37.4
874	79	9.1
955	125	8.6
1033	120	5.7
1112	78	11.1
1250-1750 cm^{-1} region		
1359	35	13.4
1381	82	39.0
1462	135	19.0
1632	84	28.5
2700-3800 cm^{-1} region		
2938	218	5.4
3266	329	30.0
3471	244	64.6

Table 4. Band component analysis of the Raman spectra of hydrotalcites with various Mg/Zn/Al ratios.

	Mg/Zn/Al 6/0/2	Mg/Zn/Al 4/2/2	Mg/Zn/Al 2/4/2
400-800 cm^{-1} region			
Bandposition (cm^{-1})		452	443
Bandwidth (cm^{-1})		41	44
% Rel. area		11.2	8.3
Bandposition (cm^{-1})	476	476	477
Bandwidth (cm^{-1})	29	31	36
% Rel. area	13.2	19.1	28.5
Bandposition (cm^{-1})		496	494
Bandwidth (cm^{-1})		16	18
% Rel. area		2.6	3.8
Bandposition (cm^{-1})	552	548	550
Bandwidth (cm^{-1})	18	25	21
% Rel. area	68.1	57.5	51.9
Bandposition (cm^{-1})	694	694	695
Bandwidth (cm^{-1})	22	24	17
% Rel. area	5.5	2.3	1.4
800-1300 cm^{-1} region			
Bandposition (cm^{-1})		879	
Bandwidth (cm^{-1})		11	
% Rel. area		1.5	
Bandposition (cm^{-1})	979	979	981
Bandwidth (cm^{-1})	13	13	12
% Rel. area	1.2	19.0	23.8
Bandposition (cm^{-1})	1053	1044	1056
Bandwidth (cm^{-1})	28	59	31
% Rel. area	42.7	21.7	32.8
Bandposition (cm^{-1})	1061.1	1060	1061
Bandwidth (cm^{-1})	9.6	11	9
% Rel. area	56.0	57.9	43.4
2700-3800 cm^{-1} region			
Bandposition (cm^{-1})	3097	3006	3068
Bandwidth (cm^{-1})	242	297	301
% Rel. area	16.3	18.2	9.5
Bandposition (cm^{-1})	3245	3261	3249
Bandwidth (cm^{-1})	189	267	210
% Rel. area	22.5	36.8	42.1
Bandposition (cm^{-1})	3358	3362	3365
Bandwidth (cm^{-1})	121	126	109
% Rel. area	17.8	16.1	15.5
Bandposition (cm^{-1})	3454	3444	3445
Bandwidth (cm^{-1})	128	118	106
% Rel. area	40.1	23.0	27.4
Bandposition (cm^{-1})	3580	3562	3535
Bandwidth (cm^{-1})	55	97	116
% Rel. area	3.4	3.5	5.5

Figure captions

Figure 1. XRD patterns of Mg/Zn/Al-hydrotalcites with various Mg/Zn ratios.

Figure 2. Band component analysis of the FT-IR spectrum of synthetic hydrotalcite with composition $Mg_4Zn_2Al_2(OH)_{16}CO_3.nH_2O$ in (a) the 390-460 cm^{-1} region, (b) the 500-1250 cm^{-1} region, (c) the 1250-1750 cm^{-1} region and (d) the OH-stretching region.

Figure 3a. Raman spectra of synthetic hydrotalcite with Mg/Zn ratios of (a) 6/0, (b) 4/2, and (c) 2/4 in the region 400-750 cm^{-1}.

Figure 3b. Raman spectra of synthetic hydrotalcite with Mg/Zn ratios of (a) 6/0, (b) 4/2, and (c) 2/4 in the region 900-1150 cm^{-1}.

Figure 4. Band component analysis of the Raman spectrum of hydrotalcite with Mg/Zn ratio 2/4 in (a) the 400-625 cm^{-1} region and (b) the 2700-3700 cm^{-1} region.

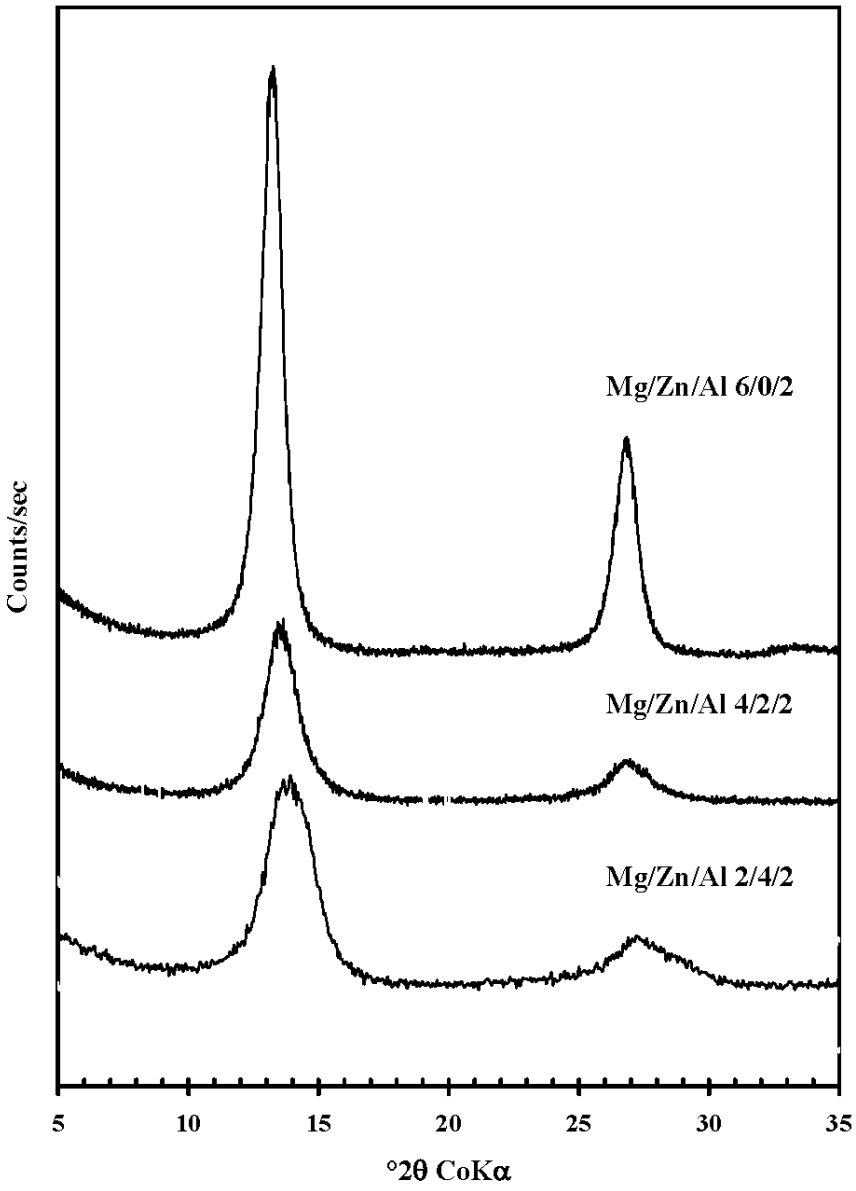

Fig. 1 X-ray diffraction patterns for Mg, Zn, Al hydrotalcites of various ratios

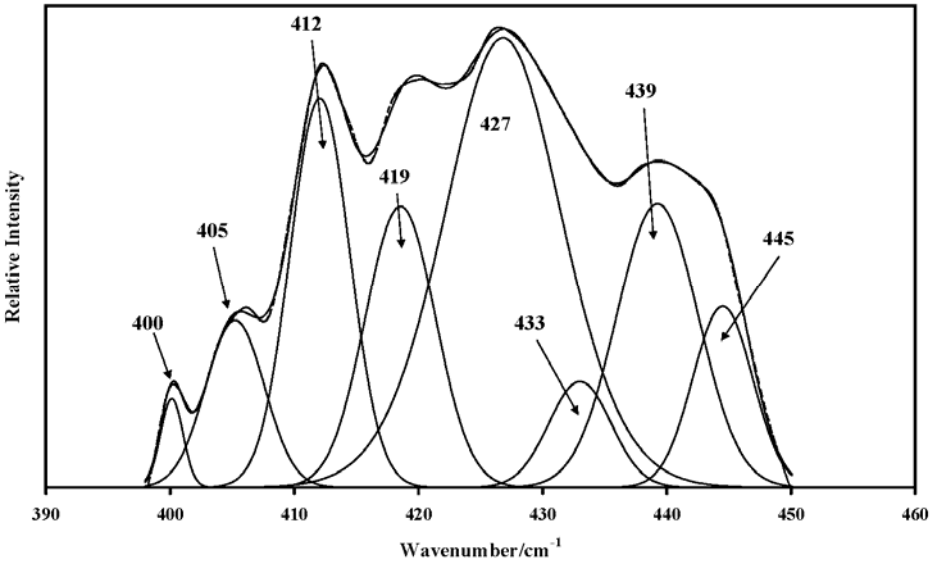

Figure 2a. Band component analysis of the FT-IR spectrum of synthetic hydrotalcite $Mg_4Zn_2Al_2(OH)_{16}CO_3.nH_2O$ in the 400-450 cm^{-1} region.

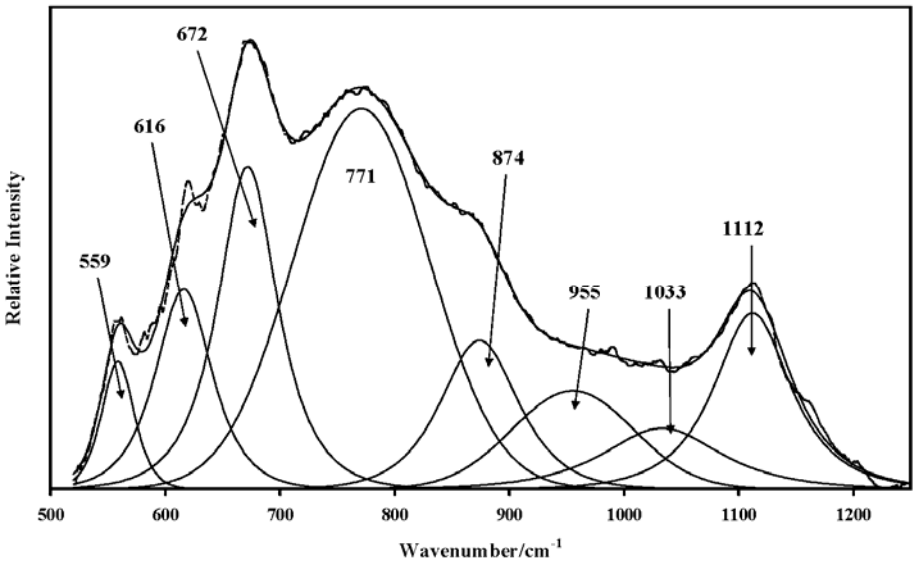

Fig. 2b. Band component analysis of the FT-IR spectrum of synthetic hydrotalcite $Mg_4Zn_2Al_2(OH)_{16}CO_3.nH_2O$ in the region 500-1250 cm^{-1}.

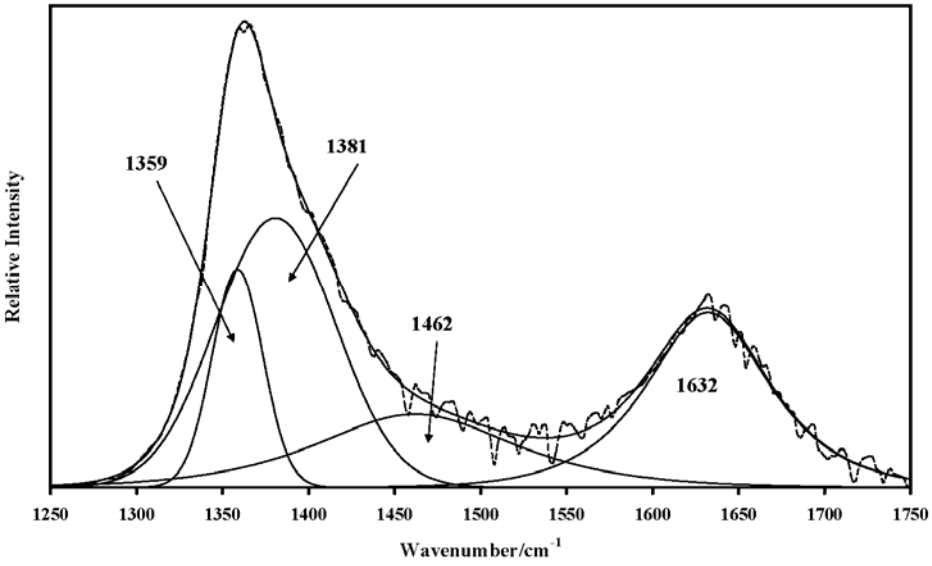

Figure 2c. Band component analysis of the FT-IR spectrum of synthetic hydrotalcite $Mg_4Zn_2Al_2(OH)_{16}CO_3.nH_2O$ in the region 1250-1750 cm^{-1}.

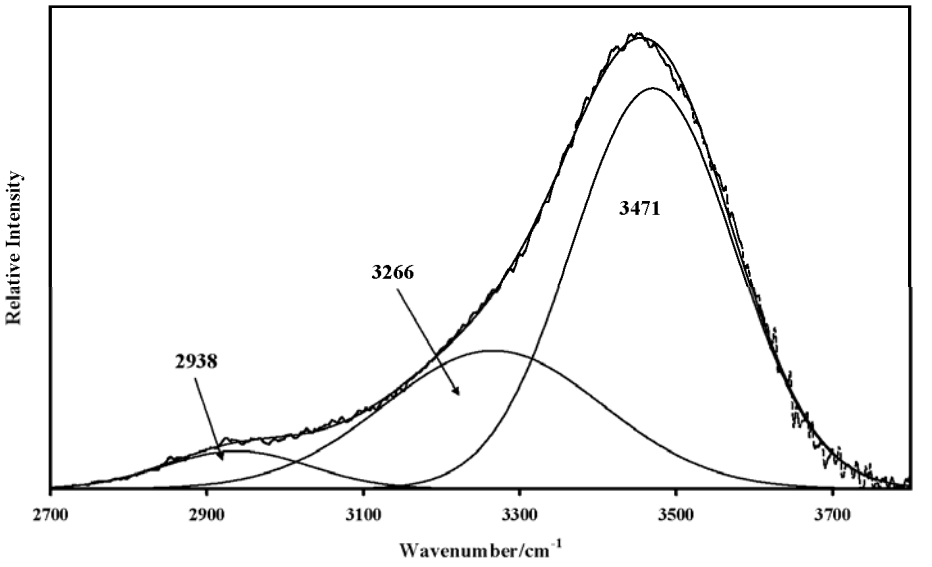

Figure 2d. Band component analysis of the FT-IR spectrum of synthetic hydrotalcite $Mg_4Zn_2Al_2(OH)_{16}CO_3.nH_2O$ in the OH stretching region.

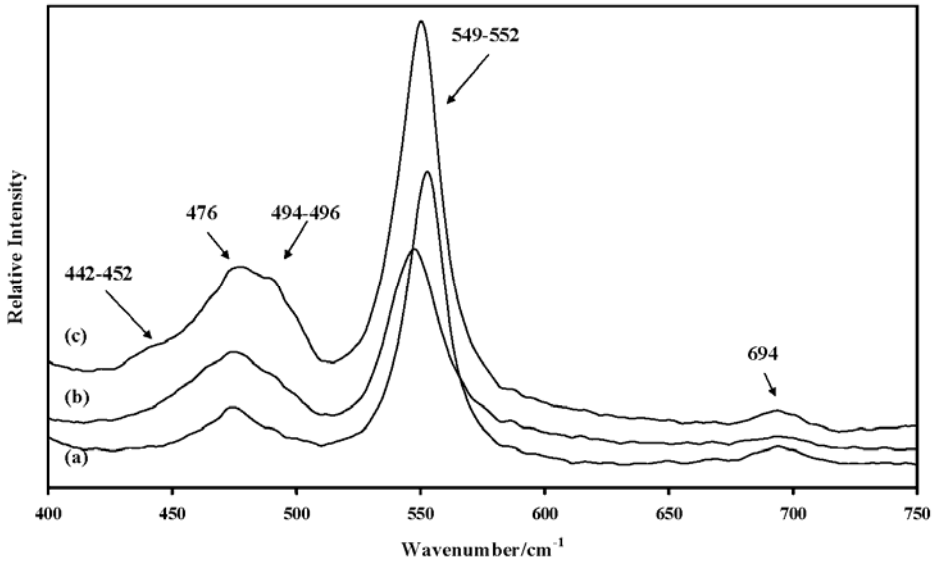

Fig. 3a. Raman spectra of synthetic hydrotalcite with Mg/Zn ratios of (a) 6/0, (b) 4/2, and (c) 2/4 in the region 400-750 cm^{-1}.

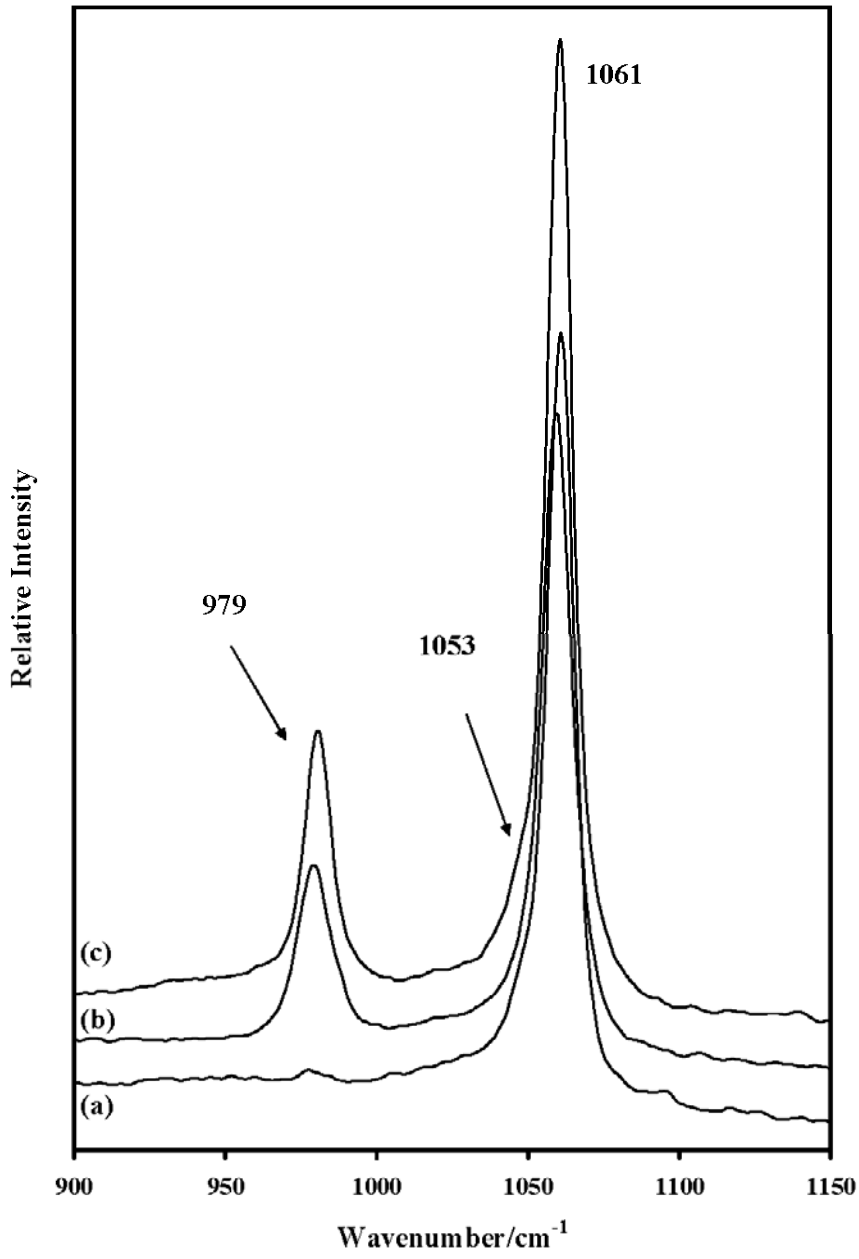

Fig. 3b. Raman spectra of synthetic hydrotalcite with Mg/Zn ratios of (a) 6/0, (b) 4/2 and (c) 2/4 in the region 900-1150 cm $^{-1}$.

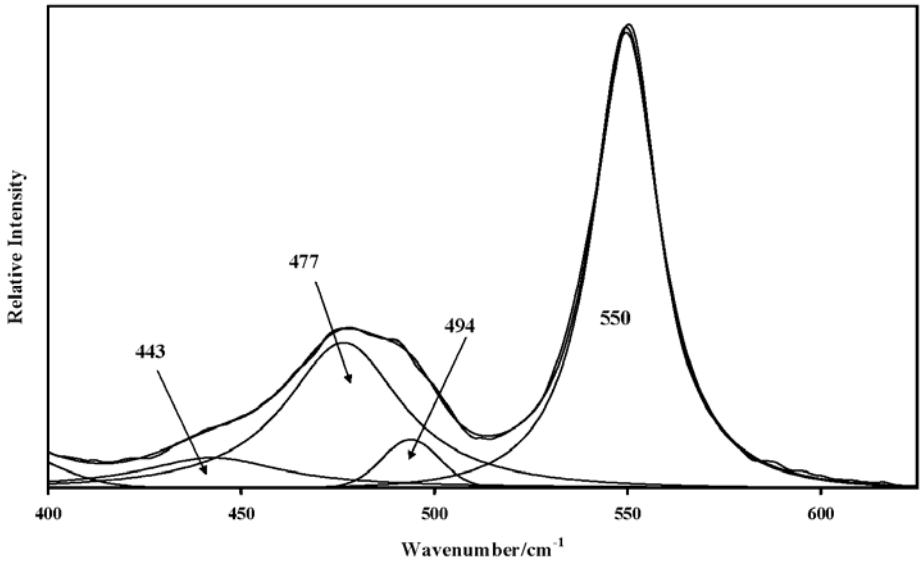

Fig. 4a. Band component analysis of the Raman spectrum of hydrotalcite Mg/Zn 2/4 in the 400-625 cm^{-1} region.

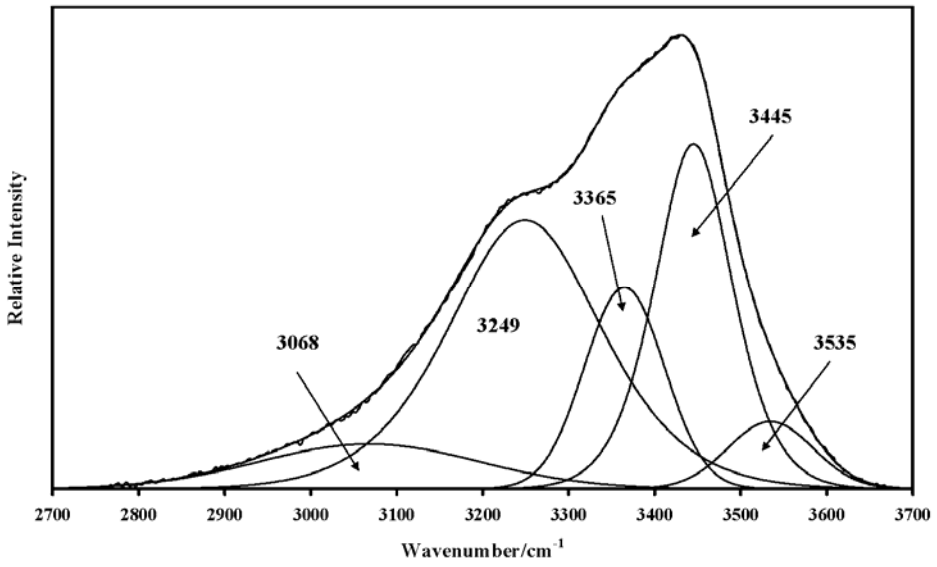

Fig. 4b. Band component analysis of the Raman spectrum of hydrotalcite Mg/Zn 2/4 in the 2700-3700 cm^{-1} region.